Carbon Letters (2022) 32:987–998
https://doi.org/10.1007/s42823-022-00332-y

Online ISSN 2233-4998
Print ISSN 1976-4251

ORIGINAL ARTICLE

Influence of carbon nanotube inclusions to electrical, thermal, physical and mechanical behaviors of carbon-fiber-reinforced ABS composites

Alinda Oyku Akar[1] · Umit Hakan Yildiz[2,3] · Seha Tirkes[4] · Umit Tayfun[3,5] · Ferda Hacivelioglu[6]

Received: 28 January 2022 / Revised: 23 February 2022 / Accepted: 1 March 2022 / Published online: 22 March 2022

Abstract

Acrylonitrile–butadiene–styrene (ABS) terpolymer was compounded with short carbon fiber (CF) and carbon nanotube (CNT) using a micro-extruder followed by the injection molding process. Composite samples were fabricated with loading ratios of 20 wt.% CF and 0.1, 0.5 and 1.0 wt.% of CNT. Mechanical, electrical, thermo-mechanical, thermal, melt-flow, and structural investigations of ABS-based composites were conducted by performing tensile, impact, hardness, and wear tests, conductive atomic force microscopy (AFM), dynamic mechanical analysis (DMA), thermal gravimetric analysis (TGA), melt flow rate test (MFR), scanning electron microscopy (SEM) characterization techniques, respectively. According to mechanical test data of resultant composites including tensile and impact test findings, CNT additions led to the remarkable increase in tensile strength and impact resistance for CF reinforced ABS composites. The formation of synergy between CNT nanoparticles and CF was confirmed by electrical conduction results. The conductive path in ABS/CF composite system was achieved by the incorporation of CNT with different loading levels. SEM micrographs of composites proved that CNT nanoparticles exhibited homogeneous dispersion into ABS matrix for lower loadings.

Graphical abstract

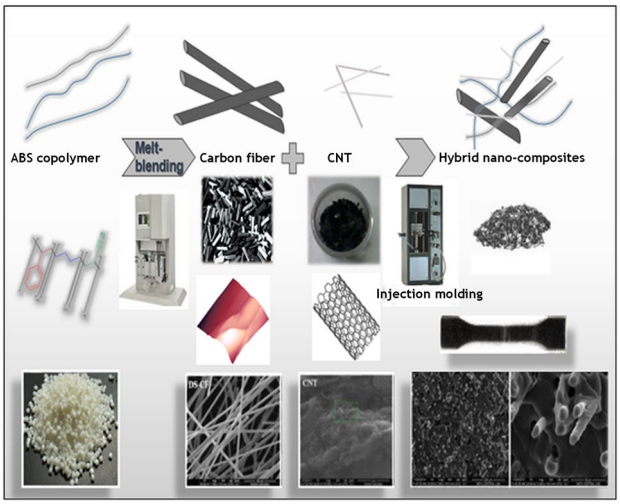

Keywords Carbon nanotube · Carbon fiber reinforced polymers · Acrylonitrile–butadiene–styrene · Polymer composites

✉ Umit Tayfun
utayfun@bartin.edu.tr

✉ Ferda Hacivelioglu
ferda@gtu.edu.tr

Extended author information available on the last page of the article

1 Introduction

The polymers are finding their way deep inside most of the applications primarily because of low weight, price, and relatively better application properties. One of the oldest and biggest application areas among others is the automotive industry. Currently, of the many parts in a vehicle, out of which 1/3 are made of plastic. Acrylonitrile–butadiene–styrene terpolymer (ABS) is one of these engineering plastics and it is being used in different automotive parts such as lightening, instrument panel, bumper, seating, door handles, interior trim, and dashboard parts [1–3].

Carbon fiber is the most desired candidate to consider as a reinforcing material for plastics because of its high mechanical properties and ease of processability. Polymer composites with carbon fiber inclusions have widespread applications in military, industrial and commercial fields; usually to shield the electromagnetic waves, and thus, allow them to work properly [4, 5]. However, higher loadings of CF to increase the conductivity of polymer composites has a detrimental effect on the mechanical and tribological performance. ABS terpolymer containing carbon fiber (CF) is one of the potential materials to become an industrial solution to achieve demanded limits, such as electrical conductance, ohmic heating, electromagnetic (EMI) shielding, and electrostatic discharge performances [6–11]. The number of research topics based on investigations of properties of ABS and its composites has been extended remarkably in the recent decade due to high interest for its application fields in 3D printing technology [12–17].

Carbon nanotube (CNT) is a member of the carbon nanostructures family that has a one-dimensional structure. The research attempts related to the structure–property relationship of CNT based on macromolecular chemistry open ways to develop CNT-reinforced polymeric materials with extraordinary properties [18–21]. Research studies regarding the use of CNT as a nano-additive for ABS-based composites were conducted for the main purpose of donating electrical conductivity to polymer structure in addition to mechanical and thermal resistance. In this regard, ABS terpolymer was compounded with CF and its related performances were investigated in the literature [22–30].

The novelty of this study lies in the establishment of synergistic interactions between two carbon-based additives into ABS phase through mechanical, thermal, and electrical behaviors. One of those additives is in micron size and fiber form while the other is nano-sized with a tubular shape. The influence of the working mechanism of these two different scales (micron and nano size) was investigated in hybrid form compared with the individual addition of CF. In the scope of this study, the effect of the CNT inclusions on CF reinforced ABS based on the mechanical, morphological, thermo-mechanical, melt-flow, electrical, and thermal properties were reported. Characterizations of fabricated composite samples were performed by tensile, impact, and Shore hardness tests as mechanical property, dynamic mechanical analysis (DMA) as a thermo-mechanical response, wear test as tribological resistance, thermogravimetric analysis (TGA) as thermal stability, atomic force microscopy (AFM) as topography, nano-mechanics, and electrical conductivity, melt flow index measurements (MFI) as rheological behaviour and scanning electron microscopy analysis (SEM) as the morphology of composites.

2 Materials and methods

2.1 Materials

Injection grade ABS was supplied from Lanxess (Cologne, Germany) with the trade name of Lustran® ABS M203FC. It has a density and hardness of 1.05 g/cm^3 (at 23 °C) and 110 N/mm^2 (ISO 2039–1, Ball indentation hardness), respectively. CF was obtained in chopped form with 3 cm polyurethane-sized strands under the trade name Aksaca, AC 0101 (Dowaksa, Yalova, Turkey). Multiwall carbon nanotube (MWCNT) was purchased from Nanocly SA, Belgium with the commercial name NC7000. The chemical oxidation process was applied to CNT using similar oxidation routes in the literature [31–33] for purification purposes.

2.2 Fabrication of composites

ABS pellets were dried at 100 °C in an oven for 2 h to evaporate the moisture content from the polymer before the processing steps.

The preparation stages of composites were carried out using a twin-screw co-rotating micro-compounder (MC 15 HT, Xplore Instruments). ABS copolymer was compounded with the loading ratios of 20 wt.% CF and 0.1, 0.5 and 1.0 wt.% of CNT. The selection of adding amounts of 0.1%, 0.5%, and 1.0% was made for the estimation of the material property for the lowest, moderate, and highest loading levels of CNT. Process temperature, screw speed, and mixing time were applied in melt-compounding process as 230 °C, 100 rpm and 5 min, respectively.

Dog-bone-shaped test specimens with the dimensions of $7.4 \times 2.0 \times 80$ mm^3 were prepared by a lab-scale injection molding device (Microinjector, Daca Instruments) using a barrel temperature of 235 °C, mold temperature of 80 °C, and the injection pressure of 8 bar. Injection-molded dog-bone specimens were used in the tensile test, narrow sections

of dogbone-shaped samples were cut to use in the impact test and DMA analysis, the grip sections of dog-bone samples were used in AFM studies, hardness tests and wear measurements.

2.3 Characterization methods

Topographical, nano-mechanical, and electrical characterizations of composites were examined by Nanosurf CoreAFM device using beam-shaped cantilever in a static mode which has spring constant of 0.2 N/m and tip radius of 7 nm. The grip section of dog-bone samples obtained from injection molding were indented at rates of 1 µm/s. Force–Distance curve measurements were performed with a Stad0.2LAuD static mod tip. Electrical conductivity measurements were carried out using ElectriMulti 75-G tip. Lloyd LR 30 K universal tensile testing equipment was used to investigate the tensile properties of ABS and composites. The load cell of 5 kN and a crosshead speed of 5 cm/min was applied during tensile tests. Recorded results represent an average value of three samples. The unnotched izod impact tests were carried out using the narrow section of dogbone-shaped samples by Coesfeld MT impact tester with the 4 J pendulum and a test speed of 3 m/s. Impact energy values of ABS and composites were measured. The TQC Shore Hardness device, which complies with DIN 53505, ISO 868, and ASTM D 2240, is used for hardness measurements of ABS and its composites. The wear test was applied in accordance with ASTM G133 standard using a UTS Tribometer T10 test device with 10 N load, 10 mm stroke, and a total sliding distance of 20 m back and forth. The grip section of the dogbone-shaped specimen was used on hardness and wear tests. Thermal characterizations of ABS and composites were performed using Netzsch Jupiter STA 449 F3 simultaneous TGA device. Test parameters were applied during TGA analysis including temperature range from 30 °C to 650 °C, a constant heating rate of 10 °C/min, and a constant nitrogen flow of 50 ml/min. Perkin Elmer DMA 8000 test device was utilized to determine thermo-mechanical behaviours of samples in chip form obtained by melt-compounding process using dual cantilever bending mode at the temperature range between − 30 °C and 150 °C with a heating rate of 5 °C/min at a constant frequency of 1 Hz. The test samples used in DMA analysis were obtained by cutting a layer from the gauge length section of dog-bone specimen. Melt flow measurements were applied to chip samples obtained by melt-blending stage under a standard load of 2.16 kg at 230 °C by Coesfield GmbH Meltfixer LT. Morphological characterizations of composites were examined by field emission scanning electron microscope (JSM-6400 Electron Microscope). Surfaces of fractured samples obtained from the impact test were coated with a thin layer of gold to obtain a conductive surface. SEM micrographs were taken at × 1000, × 2500, × 5000 and × 10,000 magnifications.

3 Results and discussions

3.1 Mechanical performance of composites

Tensile test parameters are listed in Table 1 and representative stress–strain curves are visualized in Fig. 1. According to tensile test findings, CF addition caused a significant increase in the tensile strength of neat ABS. It can be seen from the curves in Fig. 1 that the necking behaviour of unfilled ABS stem from its ductility characteristic turned into a brittle structure after both inclusions of CF and CNT

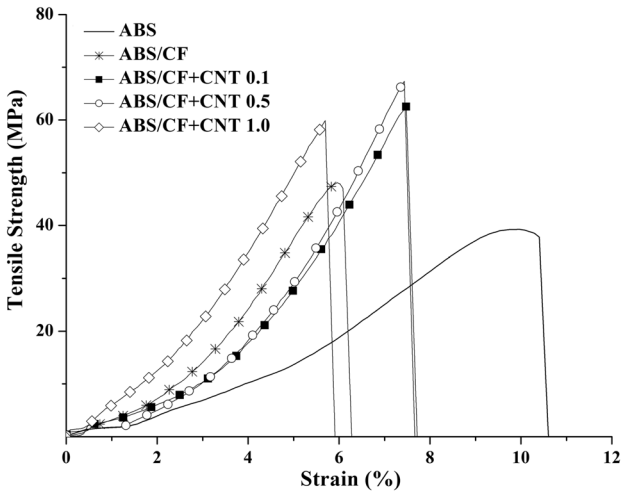

Fig. 1 Tensile curves of ABS and composites

Table 1 Tensile and hardness test data of ABS and composites

Samples	Tensile strength (MPa)	Elongation (%)	Tensile modulus (GPa)	Hardness (shore D)
ABS	39.2 ± 0.6	10.2 ± 0.5	0.71 ± 0.3	76.9 ± 0.1
ABS/CF	48.2 ± 0.5	6.2 ± 0.6	1.55 ± 0.1	77.4 ± 0.1
ABS/CF + CNT 0.1	62.7 ± 0.6	7.5 ± 0.4	1.70 ± 0.3	77.5 ± 0.1
ABS/CF + CNT 0.5	67.8 ± 0.4	7.6 ± 0.8	1.58 ± 0.1	77.7 ± 0.1
ABS/CF + CNT 1.0	60.0 ± 0.5	5.7 ± 0.8	1.54 ± 0.1	78.1 ± 0.2

in which composite samples broke down immediately as the maximum strength values were reached. The area under the stress–strain curve is related to the toughness of the material. It can be observed from Fig. 1 that composites involving CNT led to an increase in the toughness of ABS. Additionally, CNT inclusions led to obtaining higher strength values for increasing the amount of CNT up to 0.5% concentration. The amounts of improvement in tensile strength for ABS/CF + 0.5 CNT according to pristine ABS and ABS/CF samples were calculated as nearly 73% and 41%, respectively. The general trend was achieved for all of CNT inclusions in which percent elongation drop down with their filling ratios. In the case of tensile modulus results, the modulus value of unfilled ABS was enhanced by CF addition as expected. Moreover, ABS/CF + CNT ternary composites showed remarkable improvement in tensile modulus compared to ABS/CF. ABS/CF + CNT 0.1 sample gave the highest modulus value among composites. The reduction of tensile modulus with the further addition of CNT might be stem from the decrease in the dispersion homogeneity of CNT into ABS phase. As a performance comparison with previous works regarding CNT-filled ABS composites [24, 25], ABS/CF + CNT composite system exhibited superiority based on tensile properties.

According to Shore hardness data of ABS and composites listed in Table 1, CF addition caused a slight increase in Shore hardness value of neat ABS. Moreover, CNT inclusions led to improvement in the Shore hardness parameter of composites. The positive effect of carbonaceous additives on polymeric materials was also reported in the literature since these carbon-based materials donated resistance to penetration in polymer structure [34–36].

Impact test findings of ABS and its composites are illustrated in Fig. 2. Impact energy results were found to be in correlation with tensile test findings in which CF and CNT incorporations caused significant enhancement for fracture toughness of ABS. CNT-containing composites displayed similar results with CF-reinforced ABS composites. 0.1% loading level of CNT yielded the highest impact performance among composite samples, whereas, the nearly identical value was reached for ABS/CF + 0.5% CNT. According to impact test data, impact strength values decreased slightly with further additions of CNT. The reduction trend by high loadings of CNT can be explained by the restriction of deformation ability of ABS chains which resulted in a decrease in the total free energy of composite structure [16, 37–39].

3.2 Wear resistance of composites

The depth versus width curves regarding wear deformation of ABS and composites are displayed in Fig. 3 and their tribological parameters including wear volume and specific wear rate are listed in Table 2. Based on these results, it can be said that unfilled ABS and CF-reinforced ABS gave nearly identical wear performance. Wear volume and specific wear rate value of ABS/CF showed an

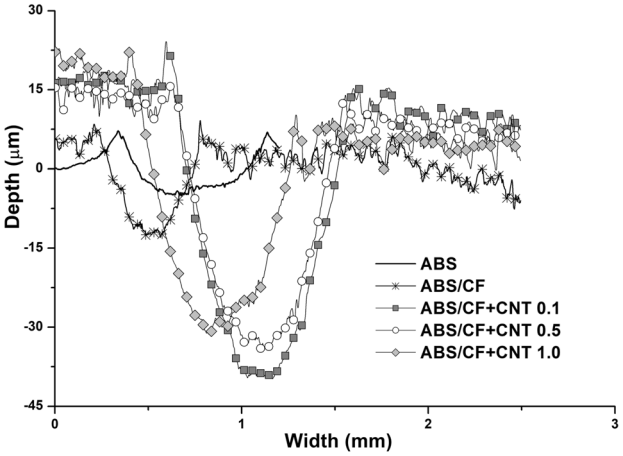

Fig. 3 Wear test curves of ABS and composites

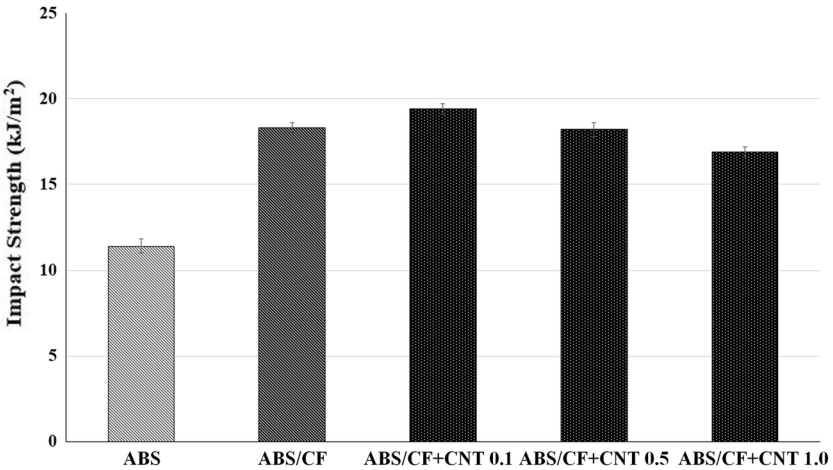

Fig. 2 Impact test results of ABS and composites

Table 2 Summary of the tribological properties of ABS and composites

Samples	Wear volume W (mm^3)	Specific wear rate W_R (mm^3/Nm)
ABS	0.067 ± 0.02	0.083 ± 0.01
ABS/CF	0.072 ± 0.08	0.090 ± 0.03
ABS/CF + CNT 0.1	0.256 ± 0.01	0.320 ± 0.02
ABS/CF + CNT 0.5	0.224 ± 0.03	0.280 ± 0.04
ABS/CF + CNT 1.0	0.202 ± 0.06	0.253 ± 0.07

increasing trend after the additions of CNT which means CNT inclusions caused a negative effect in abrasion resistance performance of composites. The tubular structure of CNT might be the main reason for the decrease in abrasion resistance. Generally, additives that have plate-like structures such as graphene led to improve in abrasion resistance [40]. However, wear deformation was found to be reduced with the increase in adding the amount of CNT which may be attributed to the stiffening effect of nanotubes. Similar results were found in the literature in which polymer composites displayed better wear performance as the amount of additive increased [41–43].

3.3 Thermo-mechanical behaviour of composites

Dynamic mechanical properties of composites were examined with the help of storage modulus, loss modulus and tan δ curves with respect to the temperature which are given in Fig. 4. The sharp lowering in the storage modulus curve is related to glass transition temperature (T_g) during the relaxation stage of the polymer chains throughout thermal transition [44, 45]. Storage modulus of ABS was found to be extended up as filled with both CNT and CF which are actively engaged in mechanical test results. Composites involving CNT displayed higher storage modulus compared to CF-reinforced ABS. The greatest modulus value was achieved for ABS/CF + 0.5% CNT sample. Similar findings for loss modulus of composites were observed. The integration of CF and CNT promoted to increase in energy dissipation which was resulted in improvement for loss modulus peak of ABS [29, 46, 47]. DMA curves indicated that T_g of ABS was not affected with the inclusion of additives regardless of their types. Tan δ curves of ABS and composites in Fig. 4 implied that the peak value of Tan δ curve of unfilled ABS stayed constant after the reinforcement with CF as opposed to CF containing composites in which lower peak values were observed since the mobility of ABS polymer chains were restricted by the high amount of CNT additive in addition to CF phase [24, 44].

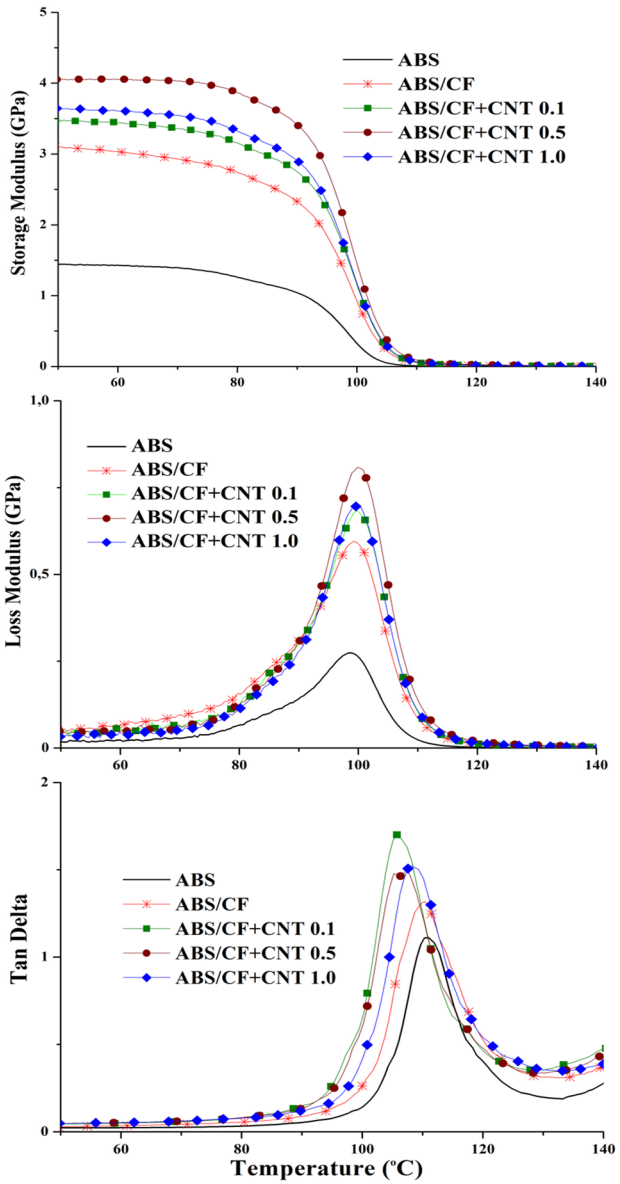

Fig. 4 DMA curves of ABS and composites

3.4 Thermal resistance of composites

The weight loss curves of ABS and composites with respect to the temperature which were obtained by TGA tests are represented in Fig. 5. Thermal decomposition of ABS terpolymer takes place in a single step in the range of nearly 380 °C to 450 °C attributed to thermal degradation of aliphatic butadiene and aromatic styrene segments in ABS chain occurs as can be observed by a sudden reduction in weight loss of ABS thermogram in indicated temperature range [48–50]. Composites incorporated with CNT exhibited a drop-down in the decomposition rate parameter of unfilled ABS. The high amount of CNT yielded a relatively more thermally stable structure compared to ABS/CF according to

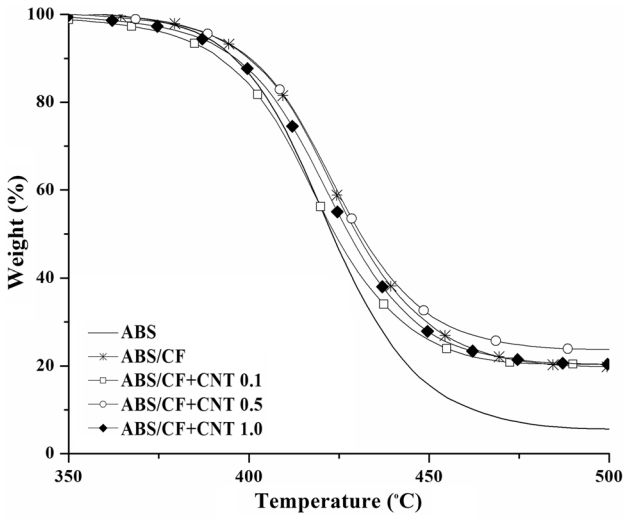

Fig. 5 TGA curves of ABS and composites

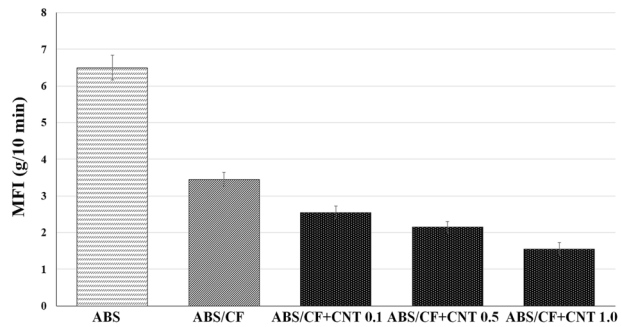

Fig. 6 MFI values of ABS and composites

TGA curves of composite samples. In other words, the lowest loading level (0.1%) of CNT inclusion caused no effect on the thermal resistance of composites. Composites filled with 0.5% CNT showed higher char yield concerning ABS and ABS/CF candidates which may be stem from the formation of thermally stable residue at the end of the analysis.

3.5 Melt-flow properties of composites

MFI test results of ABS and its composites are represented in Fig. 6. With the CF addition, MFI value of ABS was significantly reduced due to the high aspect ratio of CF. Similarly, CNT inclusion yielded the same behaviour with CF which was stem from its fibrous structure with the tubular form. Remarkable reductions in MFI parameters were observed with the increase in adding the amount of CNT which may be caused by the presence of agglomerated bundle parts of CNT particles. MFI values of CNT-filled composites were found to be in a narrow range (1.5–2.5 g/10 min). This result indicates that nearly identical process parameters can be utilized in the production stages of CNT-containing composites for additive manufacturing applications [51, 52].

3.6 AFM studies of composites

2D AFM images and cross-section graphs in Fig. 7 indicate that ABS and its composites exhibited rough surface properties. However, higher roughness values (height profile in cross-section graphs) were obtained for composite samples compared to unfilled ABS due to the presence of high amounts of CNT.

Young's modulus mapping of ABS and composites and force-distance curves are displayed in Fig. 8. Additionally, average values of pull-off force and Young modulus parameters were listed in Table 3. Young's modulus values of samples were analyzed by nano-indentation measurement with the help of the displacement of AFM tip. The distribution of Young's modulus became more homogeneous for 0.5% concentration of CNT. Additionally, higher Young's modulus values are achieved for this loading ratio for CNT compared to adding amounts of 0.1% and 1.0%. According to F-d curves displayed in Fig. 8, the maximum pull-off force of composites gave an increasing trend as the filler content increased. The upward change in slope of the force-distance curve of ABS compared to composites refers to an increase in stiffness which indicates that CNT inclusions donate stiffness to ABS structure. This finding is in correlation with impact test results in which CNT additions caused improvement in the toughness of ABS.

Figure 9 represents the current–voltage characteristics of ABS and composites which were measured from 3 different locations indicated by red squares in AFM images. According to I–V curves, the conductivity of unfilled ABS was found to be in a narrow range with a low amount of CNT which indicates that nearly no current flow was obtained. On the other hand, composites filled with 0.1% and 0.5% contents of CNT exhibited ohmic behaviour in the range obtained as more than an order of magnitude wider range of current compared to ABS which indicates that a conductive path was achieved throughout the physical connection between CNT and CF surfaces [22, 53, 54].

Conductivity measurements were performed at 128 different points in each sample and the average conductivity is shown in Fig. 10. As expected, ABS sample exhibited no conductivity whereas measurable conductivity was obtained by samples containing CF + CNT. As seen in Fig. 10, the source current increased from 0 to 30 pA as the amount of CNT increased up to 0.5% in weight. Interestingly, conductivity exhibited a sharp decrease in 1.0% CNT composition. This may be attributed to the phase separation by CF inclusion which disrupts connected CNT, providing conductive paths.

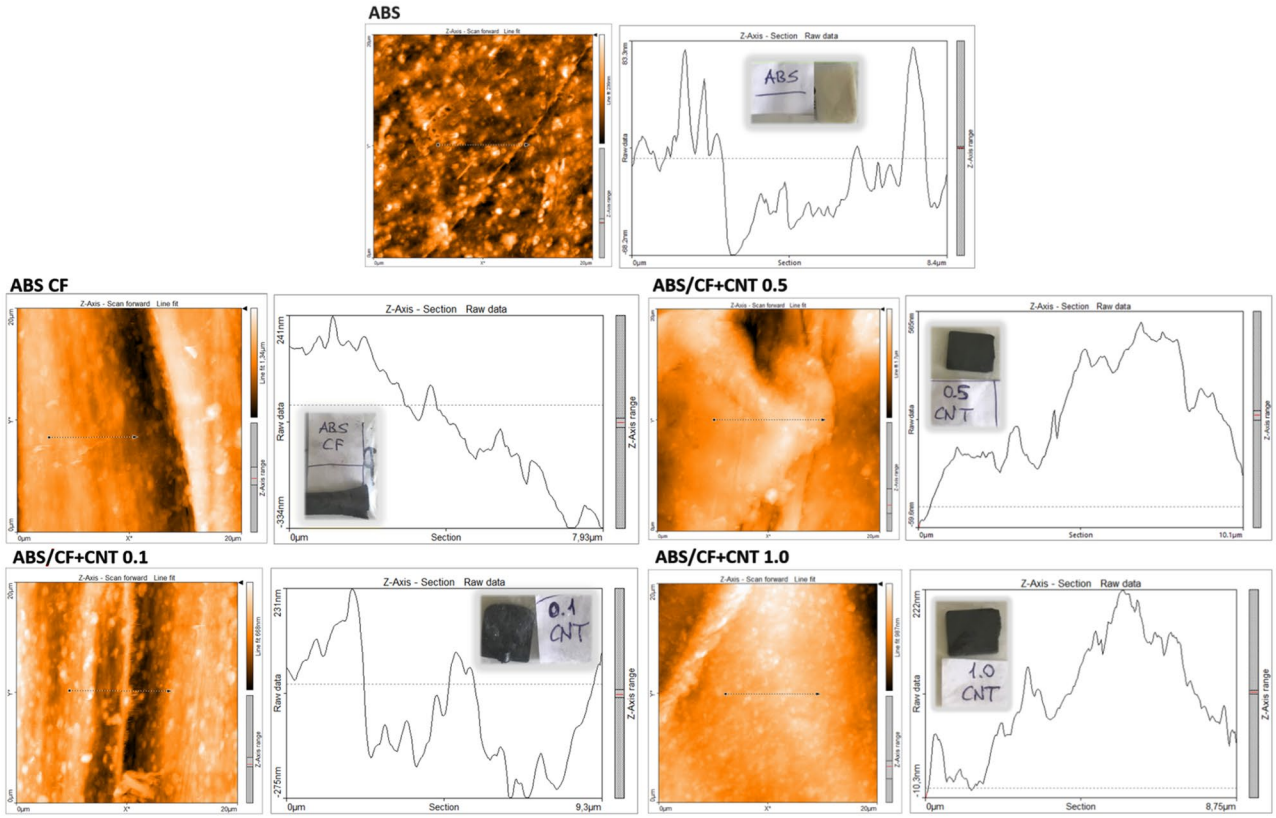

Fig. 7 Surface topography results of ABS and composites

3.7 Morphological characterization of composites

The representative SEM micrographs of composites with two different magnifications are given in Fig. 11. According to SEM images of composites, fibers were aligned in one direction for ABS/CF sample. The alignment of CFs disappeared after CNT loadings as seen in SEM images of CNT-containing composites. CNT additions also caused some debonding formations in composite structures. Nanotube domains were observed as the bundle regions for 1.0% CNT-filled composite sample. The agglomerated bundle parts were indicated by white circles in SEM images of ABS/CF + CNT 1.0 sample for more clear identification. The formation of CNT bundles in a highly loaded composite is the visual evidence of the dropping down in previously discussed performances of composites.

4 Conclusion

CNT incorporated with CF-reinforced ABS matrix at three different compositions by melt-compounding process and performances of composites were reported. Tensile test results implied that CNT inclusions led to a distinct increase in tensile strength and a slight reduction in percent elongation values. The highest tensile strength was obtained for the composite sample involving 0.5% CNT. ABS and ABS/CF gained impact resistance after the addition and CNT. Shore hardness of unfilled ABS shifted to higher levels by both inclusions of CF and CNT. Wear tests showed that CNT-filled composites exhibited poor tribological performance compared to ABS and CF-reinforced ABS. DMA analysis implied that the storage modulus and loss factor of unfilled ABS was remarkably improved after the loadings of CNT and CF. Similarly, the highest results were obtained for ABS/CF + 0.5 CNT candidate. TGA curves proved that the decomposition rate of composites was reduced by the addition of 0.5% content of CNT. Improvement of thermal resistance for ABS by the synergistic effect of CF and CNT was observed from TGA curves. MFI value of neat ABS was found to be in a reduction trend after the addition of CNT. According to AFM studies of composite samples, the maximum value and more homogeneous distributions for Young's modulus were reached as ABS/CF samples were loaded with 0.5% of CNT. Additionally, the maximum pull-out force displayed enhancement by the increase in CNT composition. Based on the conductivity characterizations by AFM, an

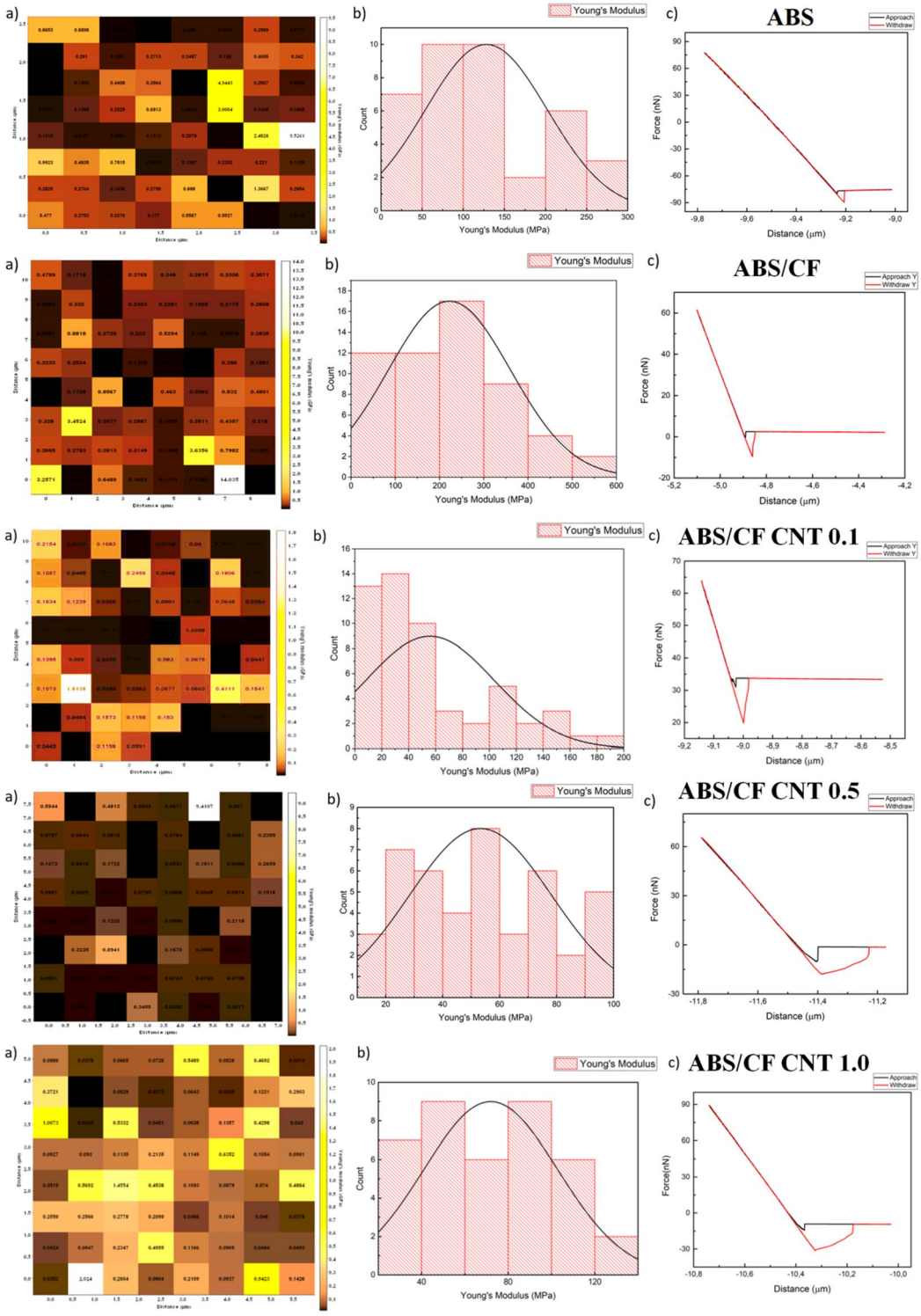

Fig. 8 Nano-mechanical analysis of ABS and composites

ohmic behaviour was obtained in the current–voltage characteristics of ABS thanks to the incorporation of CNT into non-conductive ABS structure. As the SEM micrographs of composites were examined, the high filling ratio of CNT resulted in a decrease in the homogeneity of dispersion due to the formation of bundles. Composites containing CF and a low amount of CNT exhibited morphologies with homogeneous dispersion of added fillers into ABS phase.

Table 3 Average values of pull-off force and Young modulus parameters

Samples	Average pull-off force (nN)	Average Young modulus (GPa)
ABS	165.8 ± 22.5	0.651 ± 0.018
ABS/CF	238.2 ± 19.7	1.036 ± 0.024
ABS/CF + CNT 0.1	197.3 ± 11.9	1.433 ± 0.036
ABS/CF + CNT 0.5	203.2 ± 13.6	0.962 ± 0.027
ABS/CF + CNT 1.0	199.6 ± 12.0	0.741 ± 0.032

ABS/CF + 0.5 CNT sample yielded the optimum results in the case of investigated properties since the synergistic action between CF and CNT was achieved for this loading level. As a basic conclusion remark, 0.5% amount of CNT was found to be the optimum adding ratio based on the enhanced performances of composites. The targeted application of the optimum formulation would be the transportation sector since it has multifunctional performance. CNT integrated CF reinforced ABS composite system may be a suitable option for automotive parts which is required to have thermally stable, resistance to mechanical deformations and electro-static characteristics.

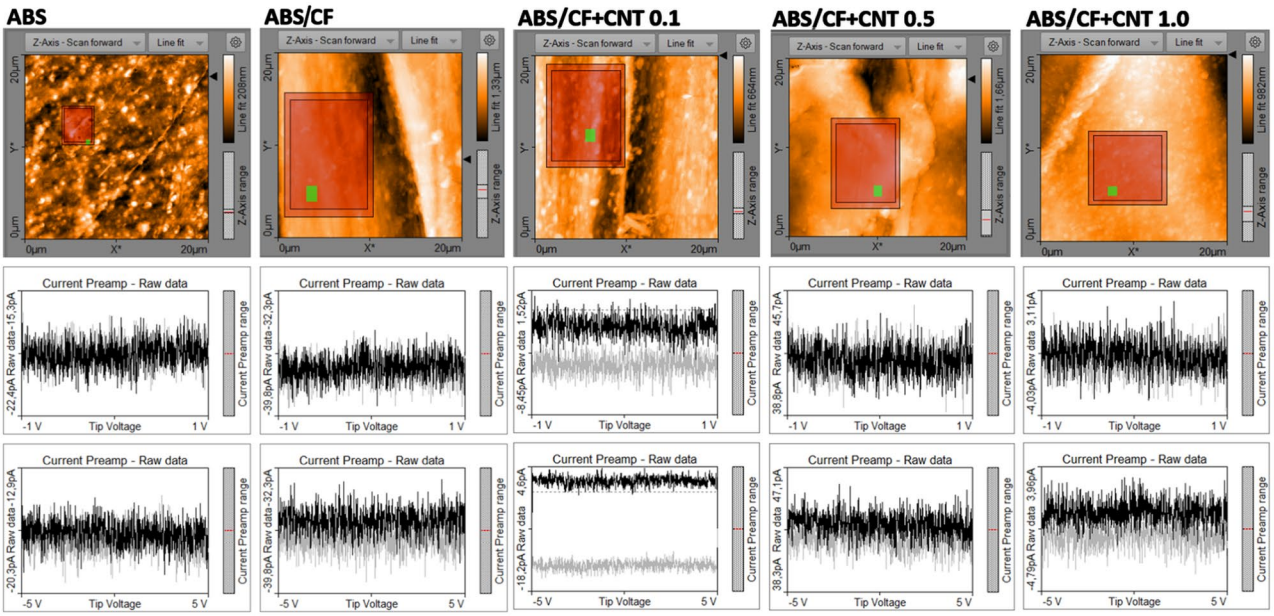

Fig. 9 Electrical conductivity results of ABS and composites

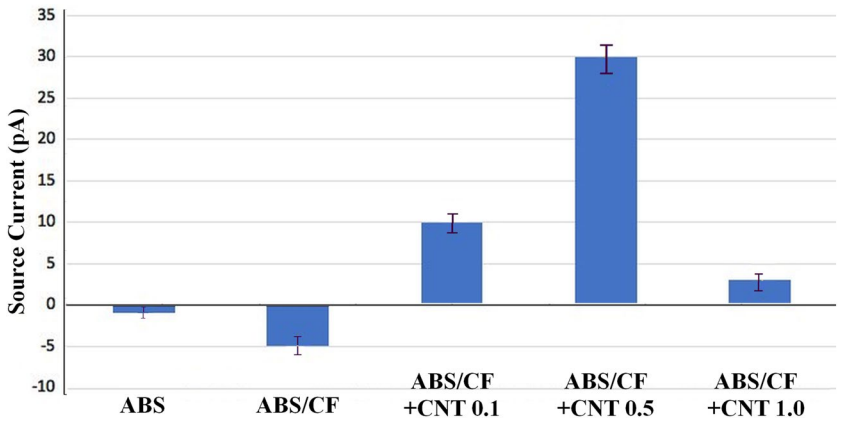

Fig. 10 Average conductivity measurements of 128 points for each sample

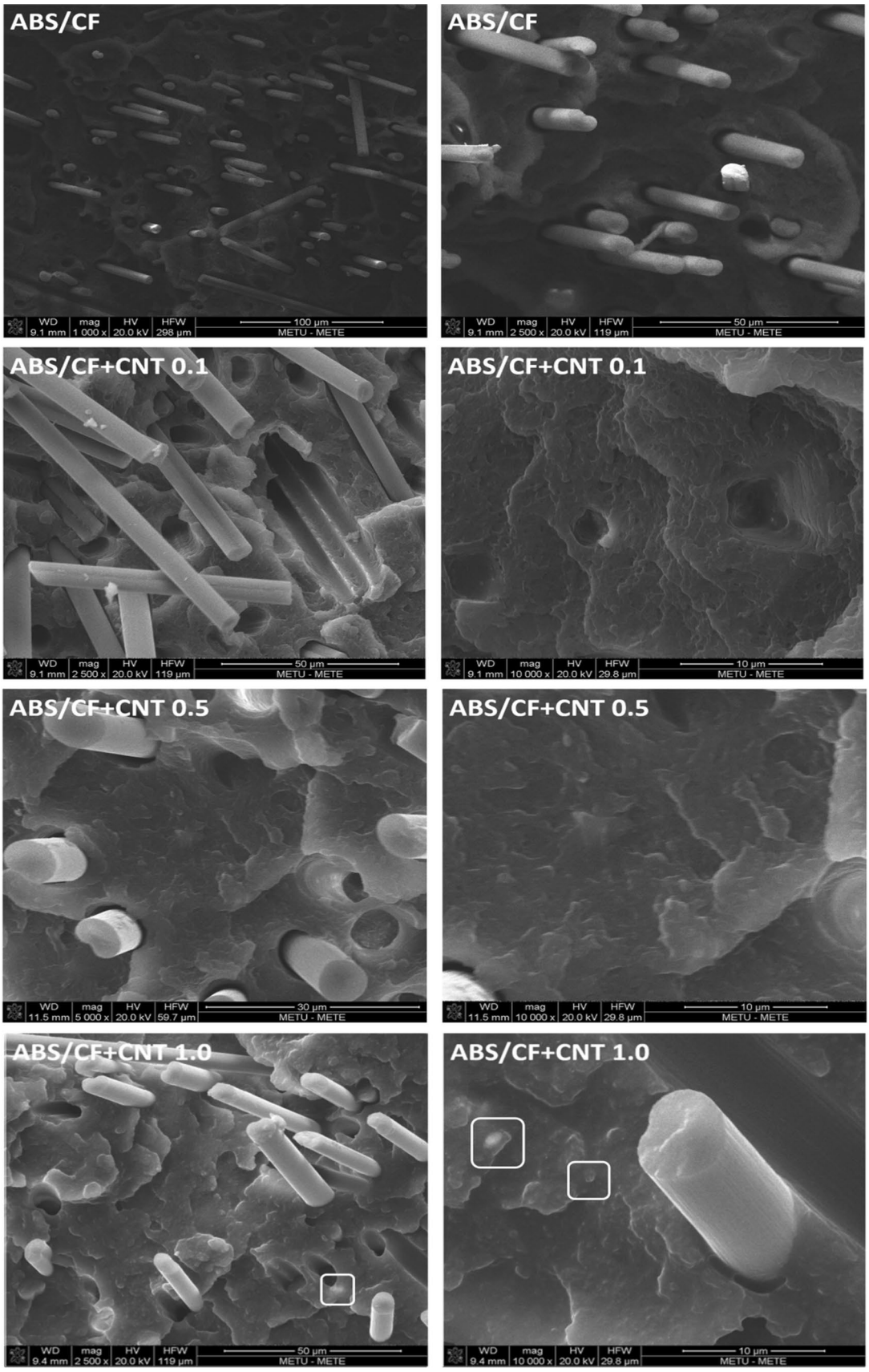

Fig. 11 SEM micrographs of composites

Declarations

Conflict of interest The authors declare that they have no conflict of interest.

References

1. Moore JD (1973) Acrylonitrile–butadiene–styrene (ABS)—a review. Compos 4:118–130
2. Mann D, Van den Bos JC, Way A (1999) Automotive plastics and composites. Elsevier Publishing, Amsterdam
3. Huang JC, Wang MS (1989) Recent advances in ABS/PC blends. Adv Polym Technol 9(4):293–299
4. Hsissou R, Seghiri R, Benzekri Z et al (2021) Polymer composite materials: a comprehensive review. Compos Struct 262:113640
5. Yao SS, Jin FL, Rhee KY et al (2018) Recent advances in carbon-fiber-reinforced thermoplastic composites: a review. Compos Part B Eng 142:241–250
6. Liang X, Ling L, Lu C et al (2000) Resistivity of carbon fibers/ABS resin composites. Mater Lett 43:144–147
7. Lu C, Xlaotlan L, Jianc H et al (1996) Electrical conductivity of carbon fibers/ABS resin composites mixed with carbon blacks. J Appl Polym Sci 62:2193–2199
8. Lu G, Li L, Jiang H (1996) Electrical and shielding properties of ABS resin filled with nickel-coated carbon fibers. Compos Sci Technol 56:193–200
9. Ogi K, Nishikawa T, Okano Y et al (2007) Mechanical properties of ABS resin reinforced with recycled CFRP. Adv Compos Mater 16:2181–2194
10. Ahmed SA, Tirkes S, Tayfun U (2020) Reinforcing effect of polyurethane sizing on properties of acrylonitrile–butadiene–styrene composites involving short carbon fiber. SN Appl Sci 2:2024
11. Yoo SH (2021) Short review of utilization of electron-beam irradiation for preparing polyacrylonitrile-based carbon fibers and improving properties of carbon-fiber-reinforced thermoplastics. Carbon Lett 32:413–429
12. Ning F, Cong W, Qiu J et al (2015) Additive manufacturing of carbon fiber reinforced thermoplastic composites using fused deposition modeling. Compos Part B Eng 80:369–378
13. Quan Z, Larimore Z, Wu A et al (2016) Microstructural design and additive manufacturing and characterization of 3D orthogonal short carbon fiber/acrylonitrile-butadiene-styrene preform and composite. Compos Sci Technol 126:139–148
14. Love LJ, Kunc V, Rios O et al (2014) The importance of carbon fiber to polymer additive manufacturing. J Mater Res 29(17):1893–1898
15. Yang C, Tian X, Liu T et al (2017) 3D printing for continuous fiber reinforced thermoplastic composites: mechanism and performance. Rapid Prototyp J 23(1):209–215
16. Tsuchikura N, Faudree MC, Nishi Y (2013) Charpy impact value of sandwich structural (CFRP/ABS/CFRP) composites constructed with carbon fiber reinforced epoxy polymer (CFRP) and acrylonitrile butadiene styrene (ABS) sheets separately irradiated by electron beam prior to lamination. Mater Trans 54:371–379
17. Huang L, Zhang Q, Wang C (2013) Interface of continuous carbon fiber reinforced ABS. J Mater Eng 3(1):30–34
18. Pang H, Xu L, Yan D et al (2014) Conductive polymer composites with segregated structures. Prog Polym Sci 39:1908–1933
19. Bokobza L (2007) Multiwall carbon nanotube elastomeric composites: a review. Polym 48:4907–4920
20. Moniruzzaman M, Winey KI (2006) Polymer nanocomposites containing carbon nanotubes. Macromol 39:5194–5205
21. Ma P, Siddiqui NA, Marom G et al (2010) Dispersion and functionalization of carbon nanotubes for polymer-based nanocomposites: a review. Compos Part A Appl Sci 41:1345–1367
22. Al-Saleh MH, Al-Anid HK, Husain YA et al (2013) Impedance characteristics and conductivity of CNT/ABS nanocomposites. J Phys D Appl Phys 46:385305
23. Schmitz DP, Silva TI, Ramoa SDA et al (2018) Hybrid composites of ABS with carbonaceous fillers for electromagnetic shielding applications. J Appl Polym Sci 135(29):46546
24. Jyoti J, Singh BP, Aryaa AK et al (2016) Dynamic mechanical properties of multiwall carbon nanotube reinforced ABS composites and their correlation with entanglement density, adhesion, reinforcement and C factor. RSC Adv 6:3997–4006
25. Dul S, Fambri L, Pegoretti A (2018) Filaments production and fused deposition modelling of ABS/carbon nanotubes composites. Nanomater 8(1):49
26. Jyoti J, Singh BP, Chockalingam S et al (2018) Synergetic effect of graphene oxide-carbon nanotube on nanomechanical properties of acrylonitrile butadiene styrene nanocomposites. Mater Res Express 5(4):045608
27. Lee D, Kim Y, Kwon OH et al (2021) Carbon fiber coating with MWCNT in the presence of polyethyleneimine of different molecular weights and the effect on the interfacial shear strength of thermoplastic and thermosetting carbon fiber composites. Carbon Lett 31(3):407–417
28. Jyoti J, Singh BP (2021) A review on 3D graphene–carbon nanotube hybrid polymer nanocomposites. J Mater Sci 56(31):17411–17456
29. Gardea F, Cole DP, Glaz B et al (2020) Energy dissipation characteristics of additively manufactured CNT/ABS nanocomposites. Rapid Prototyp J 26(3):509–517
30. Thaler D, Aliheidari N, Ameli A (2019) Mechanical, electrical, and piezoresistivity behaviors of additively manufactured acrylonitrile butadiene styrene/carbon nanotube nanocomposites. Smart Mater Struct 28(8):084004
31. Tayfun U, Kanbur Y, Abaci U et al (2017) Mechanical, electrical, and melt flow properties of polyurethane elastomer/surface-modified carbon nanotube composites. J Compos Mater 51(14):1987–1996
32. Datsyuk V, Kalyva M, Papagelis K et al (2008) Chemical oxidation of multiwalled carbon nanotubes. Carbon 46:833–840
33. Scheibe B, Borowiak-Palen E, Kalenczuk RJ (2009) Effect of the silanization processes on the properties of oxidized multiwalled carbon nanotubes. Acta Phys Polon A 116:150–155
34. Cirmad H, Tirkes S, Tayfun U (2022) Evaluation of flammability, thermal stability and mechanical behavior of expandable graphite-reinforced acrylonitrile–butadiene–styrene terpolymer. J Therm Anal Calorim 147(3):2229–2237
35. Dike AS (2020) Improvement of mechanical and physical properties of carbon fiber-reinforced polyamide composites by applying different surface coatings for short carbon fiber. J Thermoplast Compos Mater 33(4):541–553
36. Tayfun U, Dogan M, Bayramli E (2017) Polyurethane elastomer as a matrix material for short carbon fiber reinforced thermoplastic composites. Anadolu Univ J Sci Technol A Appl Sci Eng 18(3):682–694
37. Kishimoto K, Notomi M, Shibuya T (2001) Fracture behaviour of PC/ABS resin under mixed-mode loading. Fatig Fract Eng Mater Struct 24:895–903
38. Ozkoc G, Bayram G, Bayramli E (2008) Impact essential work of fracture toughness of ABS/polyamide-6 blends compatibilized with olefin based copolymers. J Mater Sci 43(8):2642–2652

39. Joynal Abedin FN, Hamid HA, Alkarkhi AF et al (2021) The effect of graphene oxide and SEBS-g-MAH compatibilizer on mechanical and thermal properties of acrylonitrile-butadiene-styrene/talc composite. Polymers 13(18):3180
40. Ozdil N, Kayseri GO, Menguc GS (2012) Analysis of abrasion characteristics in textiles. In: Adamiak M (ed) Abrasion resistance of materials. Intech, Rijeka
41. Mohamed ST, Tirkes S, Akar AO et al (2020) Hybrid nanocomposites of elastomeric polyurethane containing halloysite nanotubes and POSS nanoparticles: tensile, hardness, damping and abrasion performance. Clay Miner 55(4):281–292
42. Chan JX, Wong JF, Petru M et al (2021) Effect of nanofillers on tribological properties of polymer nanocomposites: a review on recent development. Polymers 13(17):2867
43. Karsli NG, Yilmaz T, Aytac A et al (2013) Investigation of erosive wear behavior and physical properties of SGF and/or calcite reinforced ABS/PA6 composites. Compos Part B Eng 44:385–393
44. Menard KP (2008) Dynamic mechanical analysis: a practical introduction. CRC Press, Florida
45. Savas LA, Tayfun U, Hancer M et al (2019) The flame-retardant effect of calcium hypophosphite in various thermoplastic polymers. Fire Mater 43:294–302
46. Billah KMM, Lorenzana FA, Martinez NL et al (2020) Thermomechanical characterization of short carbon fiber and short glass fiber-reinforced ABS used in large format additive manufacturing. Addit Manuf 35:101299
47. Zhang SU, Han J, Kang HW (2017) Temperature-dependent mechanical properties of ABS parts fabricated by fused deposition modeling and vapor smoothing. Int J Prec Eng Manuf 18(5):763–769
48. Suzuki M, Wilkie CA (1995) The thermal degradation of acrylonitrile-butadiene-styrene terpolymei as studied by TGA/FTIR. Polym Degrad Stabil 47(2):217–221
49. Ehrenstein GW, Riedel G, Trawiel P (2004) Thermal analysis of plastics: theory and practice. Hanser Gardner Publications, Munich
50. Polli H, Pontes L, Araujo A et al (2009) Degradation behavior and kinetic study of ABS polymer. J Therm Anal Calorim 95(1):131–134
51. Turner BN, Gold SA (2015) A review of melt extrusion additive manufacturing processes: dimensional accuracy, and surface roughness. Rapid Prototyp J 21:250–261
52. Ramanath HS, Chua CK, Leong KF et al (2008) Melt flow behaviour of poly-epsilon-caprolactone in fused deposition modelling. J Mater Sci Mater Med 19:2541–2550
53. Okutan E, Aydin GO, Hacivelioglu F et al (2013) Preparation and properties of multi-walled carbon nanotube/poly (organophosphazene) composites. J Mater Sci 48(1):201–212
54. Tu MC, Svm HK, Thilini A et al (2017) Tuning pendant groups of polythiophene on carbon nanotubes for vapour classification. Sens Actuators B Chem 247:916–922

Authors and Affiliations

Alinda Oyku Akar[1] · Umit Hakan Yildiz[2,3] · Seha Tirkes[4] · Umit Tayfun[3,5] · Ferda Hacivelioglu[6]

1 Chemical Engineering, Gebze Technical University, 41400 Kocaeli, Turkey

2 Chemistry, Izmir Institute of Technology, 34430 Izmir, Turkey

3 Inovasens Ltd, Izmir Technopark, 34430 Izmir, Turkey

4 Chemical Engineering, Atilim University, 06836 Ankara, Turkey

5 Basic Sciences, Bartın University, 74110 Bartın, Turkey

6 Chemistry, Gebze Technical University, 41400 Kocaeli, Turkey